J Vet Sci. 2022 Sep;23(5):e78
https://doi.org/10.4142/jvs.22046
pISSN 1229-845X·eISSN 1976-555X

Journal of Veterinary Science

Original Article
Pharmacology

Check for updates

Antibacterial activity of florfenicol composite nanogels against *Staphylococcus aureus* small colony variants

Jinhuan Liu [1], **Mujie Ju** [1], **Yifei Wu** [1], **Nannan Leng** [1], **Samah Attia Algharib** [3,4], **Wanhe Luo** [1,2,*]

[1]Engineering Laboratory for Tarim Animal Diseases Diagnosis and Control, College of Animal Science, Tarim University, Alar, Xinjiang 843300, China
[2]Key Laboratory of Tarim Animal Husbandry & Science Technology of Xinjiang Production & Construction Corps., Alar, Xinjiang 843300, China
[3]Department of Clinical Pathology, Faculty of Veterinary Medicine, Benha University, Moshtohor, Toukh 13736, QG, Egypt
[4]National Reference Laboratory of Veterinary Drug Residues (HZAU) and MARA Key Laboratory for Detection of Veterinary Drug Residues, Huazhong Agricultural University, Wuhan, Hubei 430070, China

OPEN ACCESS

Received: Mar 4, 2022
Revised: Jul 30, 2022
Accepted: Aug 2, 2022
Published online: Sep 2, 2022

***Corresponding author:**
Wanhe Luo
Engineering Laboratory for Tarim Animal Diseases Diagnosis and Control/College of Animal Science, Tarim University, Alar, Xinjiang 843300, China; Key Laboratory of Tarim Animal Husbandry & Science Technology of Xinjiang Production & Construction Corps. Alar, Xinjiang 843300, China.
Email: luowanhe0728@163.com
https://orcid.org/0000-0002-5170-1670

ABSTRACT

Background: Florfenicol might be ineffective for treating *Staphylococcus aureus* small colony variants (SCVs) mastitis.
Objectives: In this study, florfenicol-loaded chitosan (CS)-sodium tripolyphosphate (TPP) composite nanogels were prepared to allow targeted delivery to SCV infected sites.
Methods: The formulation screening, the characteristics, *in vitro* release, antibacterial activity, therapeutic efficacy, and biosafety of the florfenicol composite nanogels were studied.
Results: The optimized formulation was obtained when the CS and TPP were 10 and 5 mg/mL, respectively. The encapsulation efficiency, loading capacity, size, polydispersity index, and zeta potential of the optimized florfenicol composite nanogels were 87.3% ± 2.7%, 5.8% ± 1.4%, 280.3 ± 1.5 nm, 0.15 ± 0.03, and 36.3 ± 1.4 mv, respectively. Optical and scanning electron microscopy showed that spherical particles with a relatively uniform distribution and drugs might be incorporated in cross-linked polymeric networks. The *in vitro* release study showed that the florfenicol composite nanogels exhibited a biphasic pattern with the sustained release of 72.2% ± 1.8% at 48 h in pH 5.5 phosphate-buffered saline. The minimal inhibitory concentrations of commercial florfenicol solution and florfenicol composite nanogels against SCVs were 1 and 0.25 μg/mL, respectively. The time-killing curves and live–dead bacterial staining showed that the florfenicol composite nanogels were concentration-dependent. Furthermore, the florfenicol composite nanogels displayed good therapeutic efficacy against SCVs mastitis. Biological safety studies showed that the florfenicol composite nanogels might be a biocompatible preparation because of their non-toxic effects on the renal tissue and liver.
Conclusions: Florfenicol composite nanogels might improve the treatment of SCV infections.

Keywords: Florfenicol; *Staphylococcus aureus* small colony variants; antibacterial activity; therapeutic efficacy; biosafety

ORCID iDs
Jinhuan Liu
https://orcid.org/0000-0003-4978-2229
Mujie Ju
https://orcid.org/0000-0003-0826-509X
Yifei Wu
https://orcid.org/0000-0002-8016-7702
Nannan Leng
https://orcid.org/0000-0002-2588-3490
Samah Attia Algharib
https://orcid.org/0000-0002-3336-2855
Wanhe Luo
https://orcid.org/0000-0002-5170-1670

Author Contributions
Conceptualization: Luo W; Data curation: Luo W; Formal analysis: Luo W; Funding acquisition: Luo W; Investigation: Luo W; Methodology: Luo W, Liu J, Wu Y, Leng N and Ju M; Project administration: Luo W; Resources: Luo W; Software: Luo W; Supervision: Luo W; Validation: Luo W; Visualization: Luo W; Writing-original draft: Luo W; Writing-review & editing: Luo W, Algharib SA.

Conflict of Interest
The authors declare no conflicts of interest.

Data Availability
The data used to support the findings of this study are available from the corresponding author upon request.

Funding
The article is financially supported by the President fund of Tarim University (TDZKSS202144) and the Program for Young and Middle-aged Technology Innovation Leading Talents (2019CB029).

INTRODUCTION

Staphylococcus aureus (*S. aureus*) seriously threatens human and animal health and leads to enormous economic losses worldwide [1]. *S. aureus* is associated with subclinical and persistent mastitis and greatly impacts the dairy industry [2,3]. The plasticity of the *S. aureus* genome promotes the development of multidrug-resistant strains, a serious health problem for dairy cows [4]. Moreover, *S. aureus* could persist in the host in the form of *S. aureus* small colony variants (SCVs) for a long time, evade the effects of antibacterial drugs, and lead to long-term and repeated mastitis infections [5,6]. The failure of treatments for dairy cow mastitis caused by SCVs is becoming increasingly prevalent [7]. Therefore, the antibiotic treatment of dairy cows' mastitis caused by SCVs becomes more and more challenging. The minimal inhibitory concentration (MIC) of florfenicol against *S. aureus* was 4 μg/mL [8]. On the other hand, florfenicol has strong antibacterial activity against SCVs causing mastitis; it may be ineffective for their treatment because of insufficient therapeutic drug concentrations and inadequate residence time in the mammary gland [9]. Thus, targeted delivery systems for florfenicol are required to enhance the therapeutic concentrations and residence time.

Nanogels are characterized by excellent structural stability and take advantage of both nanoparticles and hydrogels, such as their good response to various environmental stimuli [10-11]. Inspired by the special micro-environment of the mammary gland (e.g., pH 5.5), the responsive nanogels can improve the therapeutic drug concentrations and residence time of florfenicol and achieve targeted delivery to the infected site of SCVs [12]. Chitosan (CS) has good biocompatibility, biodegradability, and pH-responsiveness, as well as natural antibacterial properties, non-toxic characteristics, and a wide range of sources. Therefore, it has been used widely in medicine and pharmacy [13-15]. The drug was loaded on CS hydrogels to facilitate targeted delivery to the infected sites of SCVs [16,17]. This will enable the drug to reach the required drug concentration quickly in the target area, reduce the drug loss, improve the curative effect, and reduce the possible toxic and side effects of the drug on normal tissues [18,19].

In this study, CS and sodium tripolyphosphate (TPP) were used to wrap florfenicol into CS-TPP composite nanogels to improve its therapeutic concentrations and residence time, which in turn ensures targeted delivery to SCVs infected sites and is considered the major benefit of the current study (**Fig. 1**). The formulation screening, characteristics, *in vitro* release, antibacterial activity, treatment effect, and biosafety of the florfenicol-loaded CS-TPP composite nanogels were studied.

MATERIALS AND METHODS

Materials

Florfenicol solutions (10%) and florfenicol (≥ 98.0%) were provided by Chuang Xin Pharmaceutical Co., Ltd. (China) and Jinan Xinbao Star Animal Pharmaceutical Co., Ltd. (China), respectively. CS, TPP, and dimethylformamide were purchased from Dingyuan Co., Ltd (China). The Live/Dead backlight bacterial viability kit, Mueller-Hinton (MH) broth, Luria-Bertani (LB) broth, Tryptic soy agar (TSA), and phosphate-buffered saline (PBS) were obtained from Shanghai Bestbio Biotechnology Co., Ltd (China). The SCV strains were obtained from China Agricultural University (China) and characterized using the protocol reported elsewhere [20].

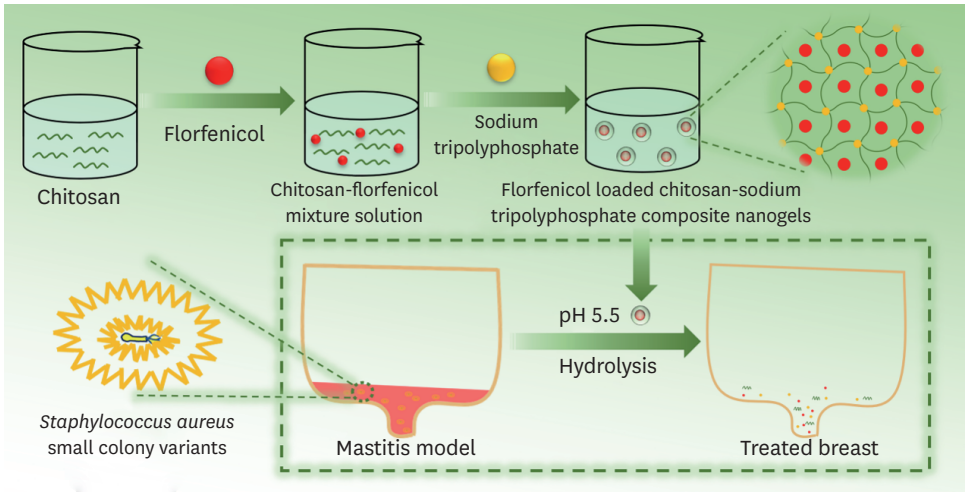

Fig. 1. Preparation process and potential release mechanisms of the florfenicol-loaded chitosan-sodium tripolyphosphate composite nanogels.

High-performance liquid chromatography (HPLC)

The florfenicol concentration was determined using a Waters 2695 series reverse-phase HPLC and performed with a detection wavelength of 225 nm at 30°C for the column. A Symmetry® C_{18} column (250 mm × 4.6 mm i.d., 5 μm) was used for separation. The mobile phase was acetonitrile and ultrapure water in the proportion of 24:76 with a mobile phase flow rate of 1 mL/min. In addition, the injection volume was 20 μL. The standard curves of florfenicol ranged from 0.1 to 50 μg/mL, $R^2 = 0.9992$ with a recovery rate > 86.5% and relative standard deviations < 8.3% for the intra-day and inter-day variation. All samples were measured three times, and the average value was taken.

Formulation of florfenicol-loaded CS-TPP composite nanogels

The florfenicol-loaded CS-TPP composite nanogels were formulated by ionic gelation. Briefly, CS (100, 200, or 400 mg; Dingyuan Co., Ltd) was added to 20 mL of a 1.0% acetic acid solution with magnetic stirring for complete dissolving. One-milliliter dimethyl formamide (Dingyuan Co., Ltd) containing 400 mg florfenicol (Jinan Xinbao Star Animal Pharmaceutical Co., Ltd) was added to 20 mL of a CS solution at 1400 RPM. Simultaneously, TPP (50, 100, 200, 400, or 800 mg; Dingyuan Co., Ltd) was dissolved in 19 mL of ultrapure water. Finally, the TPP solution was added slowly to the CS mixture solution dropwise under magnetic stirring at 1400 RPM to form florfenicol-loaded CS-TPP composite nanogels. The loading capacity (LC) and encapsulation efficiency (EE) were used to determine the optimal concentration of CS and TPP. Each sample was prepared in triplicate, and the data are expressed as mean ± SD.

Characterization

Surface morphology determination

The appearance of the optimal florfenicol composite nanogels was photographed in an inverted bottle. Furthermore, the optimal florfenicol composite nanogels were characterized by scanning electron microscopy (SEM, Hitachi S-4800; HITACHI, Japan). Briefly, 1 mg of florfenicol composite nanogels were suspended in 1 ml of distilled water, and 2 μl of the suspension was placed on a coverslip. After oven drying, the samples were coated with gold by ion sputtering and examined at an accelerating voltage of 20 kV. Subsequently, the optimal florfenicol composite nanogels were freeze-dried using a lyophilizer (FDU-1200, Japan), and freeze-dried images were evaluated by optical microscopy.

The mean size, zeta potential (ZP), and polydispersity index (PDI)

The mean size, ZP, and PDI were measured by photon correlation spectroscopy using a Zetasizer ZX3600 (Malvern Instruments, UK) at 25°C. Before the measurement, the florfenicol composite nanogels were diluted to 2.5 mg/mL by ultrapure water to obtain the optimal kilo counts per second of 20–400 for the measurements. The diameter of the particles was calculated using the Stokes–Einstein equation. All measurements were repeated three times using the samples from independent batches. The mean and SD of the triplicate measurements were reported.

In vitro release

The florfenicol composite nanogels were placed in a dialysis bag (MW: 3500) and then in 500 ml of different (pH 5.5 and 7.4) PBS at 37 ± 0.5°C. At 0.5, 1, 2, 3, 4, 6, 8, 12, 24, 36, and 48 h, 1 mL of the dialysate was taken out, and the florfenicol concentration was determined by HPLC. Thus, the cumulative release curve of florfenicol composite nanogels was drawn according to the cumulative release percentage.

Antibacterial activity studies

Determination of MICs

The MICs of florfenicol solution and florfenicol composite nanogels against SCVs were determined using the broth macrodilution method with reference to the Clinical and Laboratory Standards Institute (CLSI). Briefly, 128, 64, 32, 16, 8, 4, 1, 0.5, 0.25, 1.25, 0.625, and 0.3125 μg/ml of the florfenicol solution and florfenicol composite nanogels in MH broth (Shanghai Bestbio Biotechnology Co., Ltd) were prepared. The final concentration of the SCV strains was 5×10^5 CFU/mL. After 24 h incubation of the cultures at 37°C, the MICs of the florfenicol solution and florfenicol composite nanogels against SCVs were determined as the lowest concentration inhibiting the visible growth of bacteria. The experimental results were repeated three times.

Time-killing curves

The *in vitro* killing curves of florfenicol solution and florfenicol composite nanogels against the SCV strains were obtained by plotting time as a function of log10 CFU/mL. The SCVs strain was recovered in 3 ml LB broth (Shanghai Bestbio Biotechnology Co., Ltd), streak-inoculated on TSA, and added to 2 ml of MH broth, giving a starting inoculum of 10^6 CFU/ml. Subsequently, a serial concentration corresponding to 1/2 × MIC, 1 × MIC, 2 × MIC, and 4 × MIC of the florfenicol solution and the florfenicol composite nanogels were obtained. Finally, the bacterial count (CFU/mL) was calculated at 1, 2, 4, 8, 12, 24, 48, and 72 h, and the *in vitro* killing curves were plotted.

Live/dead bacterial staining analysis

The viability of the florfenicol solution and the florfenicol nanogels composite solution after treatment was quantified using a live/dead background viability detection kit (Shanghai Bestbio Biotechnology Co., Ltd). The SCV strains (1×10^6 CFU/mL) were treated with a serial concentration corresponding to 1/2 × MIC, 1 × MIC, 2 × MIC, and 4 × MIC of florfenicol solution and florfenicol composite nanogels for 2 h. Subsequently, all samples were treated with the live/dead backlight bacterial viability kit. Eventually, 5 μL of bacterial suspension was dropped onto the slide and evaluated by fluorescence microscopy.

Animal experiment

Mouse mastitis model

The mouse mastitis model was established using the SCV strains according to previous reports [21]. Briefly, twelve healthy Kunming species mice (18–23 g) were separated randomly into two groups (n = 6). Subsequently, 0.1 mL of SCVs containing approximately 1.2×10^9 CFU/ml was administered to each mouse to produce the mouse mastitis model. Each mouse was then inoculated orally by gavage with 0.1 mL of a 0.9% NaCl solution to construct the non-infected control group model. After inoculation, all mice were euthanized 24 h post-infection, and the mammary gland was collected aseptically. The successful establishment of the mouse infection model was determined by polymerase chain reaction (PCR) analyses [22]. All experimental protocols were carried out following the requirements of the Animal Care and Use Committee of Huazhong Agricultural University (approved number: HZAUSW-2019-009).

Treatment schedules

Thirty mice were separated randomly into the following five groups of six animals [23]: group NC 1 (non-infected control group); group IC 1 (infected control group and treated with 10 mg/mL CS solution); group IC 2 (infected control group and treated with 5 mg/ml TPP solution); group Native 1 (infected group and treated with florfenicol solution, 0.02 mL/20 g, administered by the mammary gland injection); group Native 2 (infected group and treated with florfenicol composite nanogels, 0.2 mL/20 g, administered by the mammary gland infusion). Subsequently, all mice of each group were euthanized on day 5 post-infection. In addition, the mammary gland of mice was harvested for PCR analyses on day 5. The therapeutic efficacy of the florfenicol solution and florfenicol composite nanogels on the mouse SCVs mastitis model was compared by PCR.

In vivo biosafety study

In vivo biosafety study was performed in twelve healthy Kunming mice through a breast injection with a 0.2 mL 0.9% (w/v) NaCl solution and florfenicol composite nanogels (0.2 mL/20 g). The renal and liver functions of the mice were evaluated by hematoxylin and eosin (H&E) staining and blood biochemistry analysis. Blood biochemistry analysis included the indicators of aspartate aminotransferase (AST), alanine aminotransferase (ALT), blood urea nitrogen (BUN), and creatinine (CREA).

Statistical analysis

The experimental data are expressed as mean ± SD and analyzed by one-way ANOVA using the SPSS 19.0 software (IBM Corp., USA). A *p*-value less than 0.05 was considered significant.

RESULTS

Optimization of florfenicol-loaded CS-TPP composite nanogels

The florfenicol-loaded CS-TPP composite nanogels were formulated by ionic gelation. The formulation was optimized using the CS and TPP concentrations as variables, and LC and EE as assessment indices. The EE and LC of preparation were the largest, and the optimal formula was obtained. The mean LC and EE of the florfenicol composite nanogels prepared using different CS and TPP concentrations were different (**Table 1**). When the concentrations of chitosan were the same, there was an exponential relationship, in which the LC and EE increased with increasing TPP concentrations. On the other hand, the LC and EE decreased

Table 1. Optimization of the florfenicol-loaded chitosan-sodium tripolyphosphate composite nanogels (n = 3)

Sodium tripolyphosphate (mg/mL)	Chitosan (mg/mL)	Loading capacity (%)	Encapsulation efficiency (%)
1.25	5	1.9 ± 0.3	67.3 ± 1.5
2.5	5	2.6 ± 0.4	70.5 ± 2.2
5	5	4.3 ± 0.6	84.4 ± 1.7
10	5	5.8 ± 1.4	87.3 ± 2.7
20	5	5.5 ± 0.3	83.9 ± 0.3
10	2.5	4.8 ± 0.6	83.8 ± 0.2
10	10	4.8 ± 0.2	78.4 ± 0.5

Data are presented as mean ± SD.

when the concentrations of TPP exceeded 10 mg/mL. When the concentrations of TPP were the same, however, the chitosan concentration was 5 mg/mL, and the LC and EE were the largest. Thus, the optimized formulation of the florfenicol-loaded CS-TPP composite nanogels was obtained when CS and TPP were 10 and 5 mg/mL, respectively, and the LC and EE were 5.8% ± 1.4% and 87.3% ± 2.7%, respectively.

Properties of florfenicol-loaded CS-TPP composite nanogels

The florfenicol-loaded CS-TPP composite nanogels showed homogenous transparent hydrogels in an inclined bottle, as shown in **Fig. 2A**. Interestingly, the appearance of lyophilized florfenicol-loaded CS-TPP composite nanogels displayed a uniform across-linked network by optical microscopy (**Fig. 2B**). SEM revealed a spherical shape with a relatively uniform distribution (**Fig. 2C**). The florfenicol-loaded CS-TPP composite nanogels were distributed evenly and were spherical with a smooth appearance. **Fig. 2C** showed that the particle size of the florfenicol-loaded CS-TPP composite nanogels was approximately 200 nm. The results of the lyophilized appearance and SEM images were consistent with the pattern diagram. Thus, the florfenicol-loaded CS-TPP composite nanogels had been developed. The particle size, PDI, and ZP of the optimal florfenicol composite nanogels were 280.3 ± 1.5 nm, 0.15 ± 0.03, and 36.3 ± 1.4 mv, respectively (**Fig. 2D and E**).

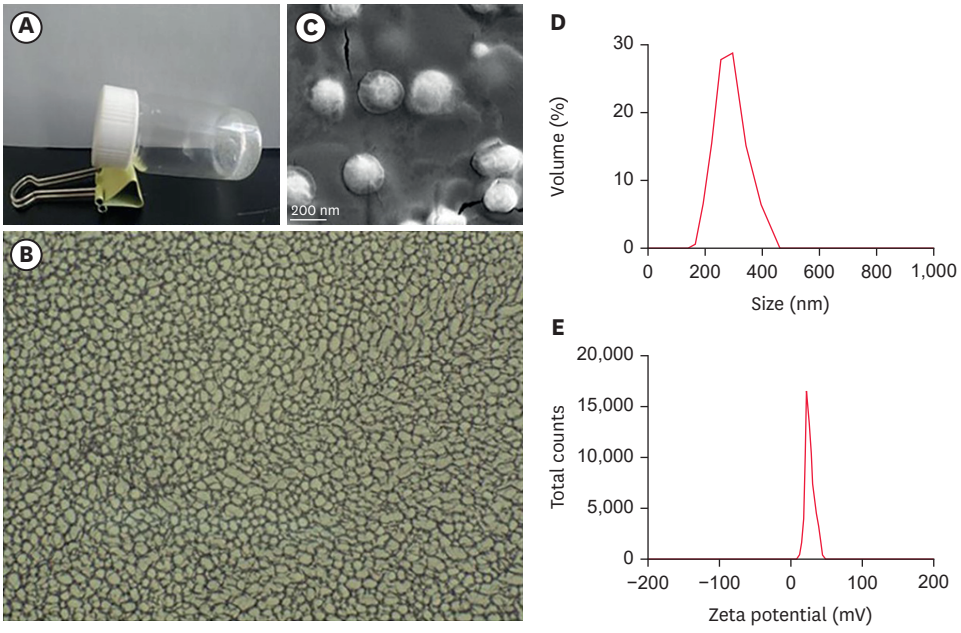

Fig. 2. Characterization of the optimal florfenicol composite nanogels: (A) photograph of an inclined bottle containing the nanogels; (B) lyophilized appearance (×800); (C) scanning electron microscopy; (D) size distribution; (E) zeta potential distribution.

https://doi.org/10.4142/jvs.22046

In vitro release study

The pH of the inflammatory sites caused by SCVs infection is usually ≂5.5 [10,11]. Therefore, the release of the florfenicol-loaded CS-TPP composite nanogels in pH 5.5 and 7.4 PBS was determined to evaluate the pH-responsive release. In pH 5.5, 72.2% ± 1.8% was released from florfenicol-loaded CS-TPP composite nanogels at 48 h, while 63.4% ± 3.1% was released in the pH 7.4 PBS at 48 h (**Fig. 3**). The *in vitro* release study showed that the florfenicol composite nanogels exhibited a biphasic pattern with sustained release in the pH 5.5 PBS. The results suggested that the florfenicol-loaded nanogels had obvious sustained-release performances and might help treat infections caused by SCVs.

Antibacterial activity

Fig. 4 presents the antibacterial activity of florfenicol solution and florfenicol composite nanogels. The MICs of florfenicol solution and florfenicol composite nanogels against SCV strains were 1 and 0.25 μg/mL, respectively. The *in vitro* time-killing curves showed that the bactericidal effect of the florfenicol solution and florfenicol composite nanogels was remarkable (**Fig. 4A and B**). The bactericidal ability of florfenicol solution and florfenicol composite nanogels also increased with increasing drug concentration. In particular, the concentration of florfenicol solution and florfenicol composite nanogels were all 2 × MIC (2 and 0.5 μg/mL), and the radical killing effects were observed. When the concentration was 2 × MIC (2 μg/mL), the florfenicol solution could completely kill the SCV strains at 48 h. Similarly, florfenicol composite nanogels could almost completely kill the SCV strains at 48 h when the concentration was 2×MIC (0.5 μg/ml). In addition, the SCV strains were processed with a florfenicol solution and florfenicol composite nanogels by live–dead staining after 2 h of incubation. Compared to the florfenicol solution group, there were fewer live SCV strains (dyed green) in the florfenicol composite nanogels (**Fig. 4C**). In particular, the florfenicol composite nanogels exhibited more potential antibacterial activity against SCVs than the florfenicol solution.

Therapeutic experiment

Compared to the non-infected control group model, the results of PCR showed that the SCVs mastitis model had been established. The mouse mastitis model was established when the bands (279 bp) were amplified by PCR in the mouse mastitis model, and no bands were amplified in the non-infected control group model (**Fig. 5A**). The cure rate was calculated to evaluate the treatment effect of florfenicol solution and florfenicol composite nanogels

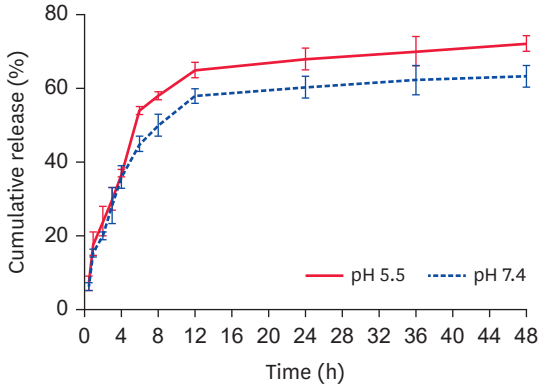

Fig. 3. *In vitro* release of florfenicol composite nanogels in different pH (5.5 and 7.4) Phosphate-buffered saline (mean ± SD, n = 3).

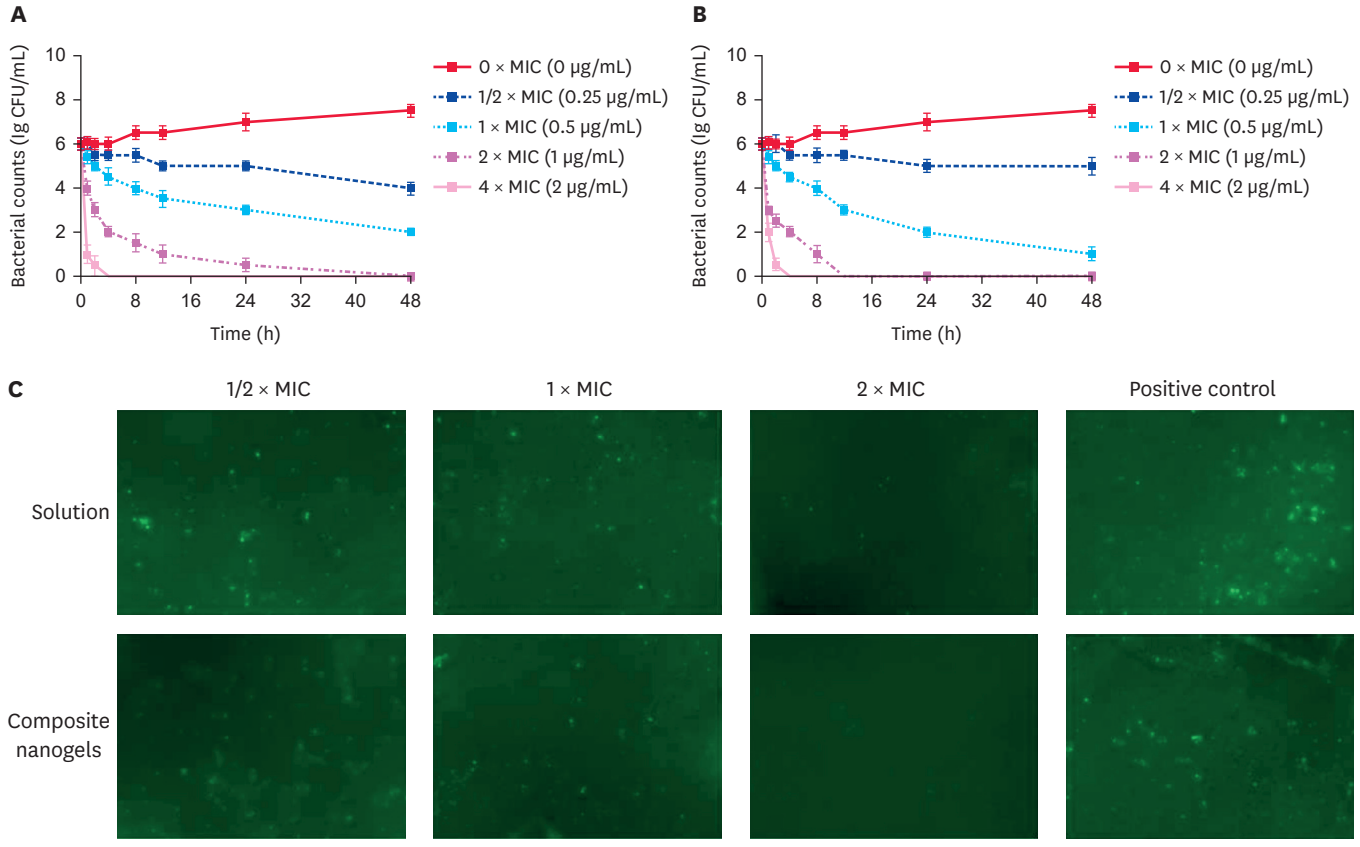

Fig. 4. Antibacterial activity of the florfenicol solution and florfenicol composite nanogels against SCVs. A-B: killing curve of florfenicol solution (A) and florfenicol composite nanogels (B) against SCV strains (n = 3) (C) number of living SCV strains incubation with florfenicol solution and florfenicol composite nanogels for 2 h.
MIC, minimal inhibitory concentration; SCV, small colony variant.

on the SCVs mastitis model. The treatment was classified into groups NC, IC 1, IC 2, Native 1, and Native 2. PCR was performed to determine if the infected mice were cured (**Fig. 5B**). The infected mice were completely cured when there were no amplified bands by PCR (279 bp). The cure rates of the groups NC, IC 1, IC 2, Native 1, and Native 2 were 100%, 10%, 0.0%, 76.6%, and 80.0%, respectively (**Fig. 5C**). CS had slight antibacterial activity, with a cure rate of only 10%. TTP had no antibacterial activity (cure rate of 0%). The cure rate of the commercial florfenicol solution (76.6%) was lower than that of florfenicol composite nanogels (80.0%), which may be due to the following: 1) CS was added to the florfenicol composite nanogels, and florfenicol and CS played an antibacterial role. 2) The florfenicol composite nanogels showed sustained-release performance, which led to an increase in cure rate. 3) The preparation of florfenicol composite nanogels enhanced the antibacterial activity of florfenicol. Hence, the same dose of florfenicol composite nanogels might have the same therapeutic efficacy as a commercial florfenicol solution.

Biosafety studies

In this study, the biosafety of the florfenicol composite nanogels was evaluated by H&E staining and *in vivo* blood biochemistry analysis. The mammary gland, liver, kidneys, and blood were collected for biosafety studies through a mammary gland injection with florfenicol composite nanogels. There was no significant pathological change in the mammary gland, liver, and renal tissues through a breast injection with the florfenicol

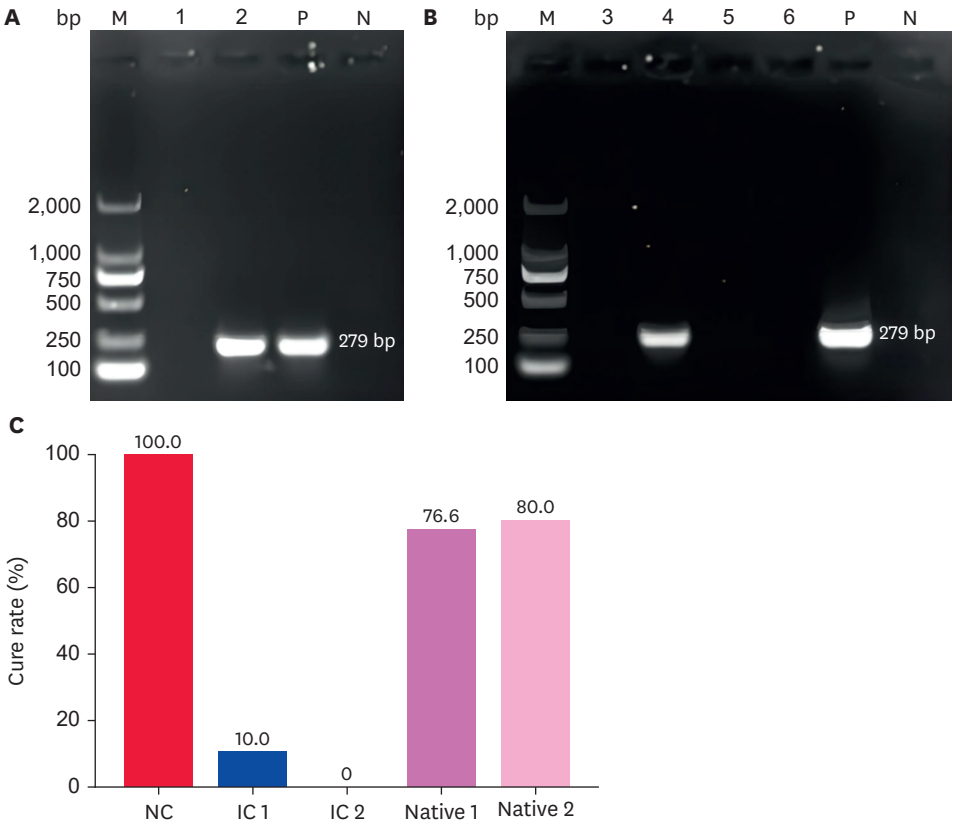

Fig. 5. Evaluation of mouse mastitis model and therapeutic efficacy in different groups.
Evaluation of mouse infection model (A) and therapeutic efficacy (B) by polymerase chain reaction; M: 2000 marker, 1: the breast sample of the non-infected control group model, 2: the mouse mastitis model, 3: the breast sample of group NC, 4: the breast sample of group IC, 5: group Native 1, 6: group Native 2, P: positive control, N: Negative control. (C) The evaluation of therapeutic efficacy in different groups.

composite nanogels relative to the control group (**Fig. 6A and D**). The blood biochemistry of all mice showed that the ALT, AST, BUN, and CREA levels were within the normal ranges in the NC, Native 1, and Native 2 groups. On the other hand, the difference was not statistically significant (**Fig. 6E and H**). These results suggest that the florfenicol composite nanogels had no toxic effects, particularly on the mammary glands, liver, kidneys, and blood.

DISCUSSION

The prepared nanogels can enhance the concentration and residence time of drugs at the infection sites, thereby improving the antibacterial effect of drugs, which has attracted increasing attention [24]. In this study, florfenicol-loaded CS-TPP composite nanogels were successfully formulated by ionic gelation. The formula of the florfenicol-loaded CS-TPP composite nanogels was optimized considering EE and LC as evaluation indicators, as well as CS and TPP concentration as variables. A higher EE and LC of the florfenicol-loaded CS-TPP composite nanogels meant successful formations of florfenicol composite nanogels [25]. The optimized formulation of the florfenicol-loaded CS-TPP composite nanogels was obtained when CS and TPP were 10 and 5 mg/mL, respectively.

https://doi.org/10.4142/jvs.22046

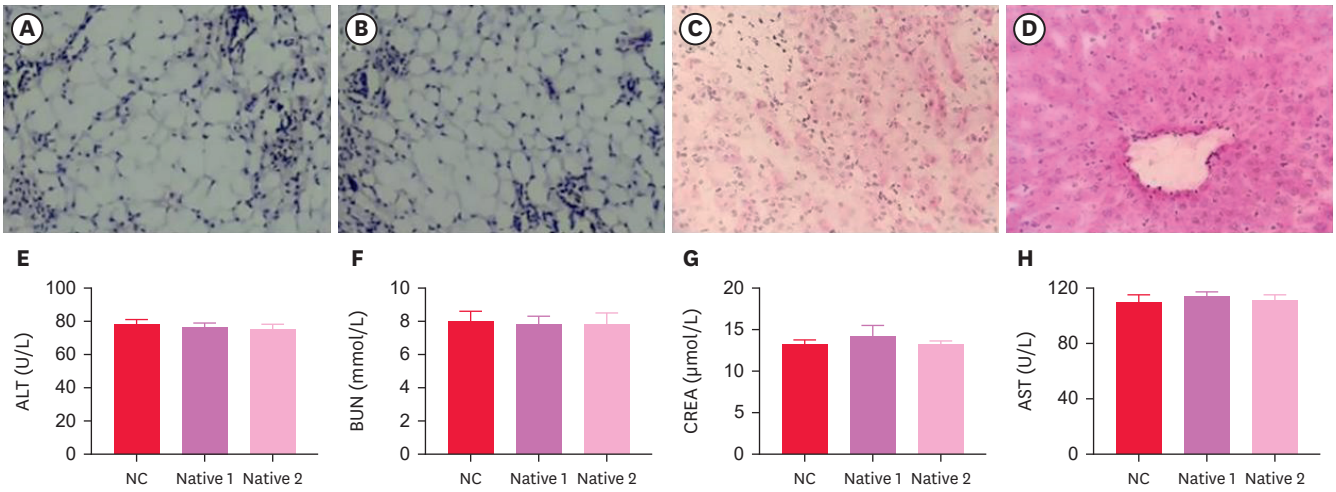

Fig. 6. Biosafety studies of florfenicol-loaded CS-TPP composite nanogels. (A) Breast of control group mice (×800). (B-D) Mammary gland, kidney, and liver of mice injected with florfenicol composite nanogels group (×800). (E-H) Blood biochemistry (ALT, AST, BUN, and CREA) in NC, Native 1 group, and Native 2 group (mean ± SD, n = 3).
ALT, alanine aminotransferase; BUN, blood urea nitrogen; CREA, creatinine; AST, aspartate aminotransferase.

The florfenicol composite nanogels did not flow and showed gelatinous consistency in an inclined bottle. The florfenicol composite nanogels were successfully formulated to a certain extent. In general, freeze-dried hydrogels displayed a network structure [25]. This phenomenon was verified by electron microscopy (uniform across-linked networks). Thus, florfenicol composite nanogels might be incorporated into a cross-linked polymeric network. This observation agrees with previous studies [26]. The SEM image (spherical with a relatively uniform distribution) was similar to another previous study [27], suggesting that the florfenicol-loaded CS-TPP composite nanogels were successfully developed by ionic gelation. The results of the lyophilized appearance and SEM images were consistent with the pattern diagram of the florfenicol-loaded CS-TPP composite nanogels.

In this study, the particle size, PDI, and ZP were 280.3 ± 1.5 nm, 0.15 ± 0.03, and 36.3 ± 1.4 mv, respectively. This showed that the florfenicol-loaded CS-TPP composite nanogels were nanoscale and dispersed uniformly. This means that drugs can pass through bacterial cell membranes easily and kill bacteria. Interestingly, florfenicol-loaded nanogels with a positive charge could have a more substantial bactericidal effect through electrostatic interactions with the bacterial membrane with a negative charge. Nano-drugs can improve the bioavailability of drugs and allow targeted and sustained release [28]. The *in vitro* release study showed that florfenicol composite nanogels exhibited a biphasic pattern with sustained release in pH 5.5 PBS. Therefore, the *in vitro* release showed that the prepared florfenicol-loaded CS-TPP composite nanogels had targeted and sustained release, which had great advantages in treating SCV infection.

The antibacterial activity was evaluated by MICs, time-killing curves, and live/dead bacterial staining analysis to determine if the florfenicol composite nanogels have a stronger bactericidal effect than a commercial florfenicol solution. The MICs showed that the florfenicol composite nanogels (0.25 μg/mL) could enhance the susceptibility to florfenicol compared to the florfenicol solution (1 μg/mL). Hence, the antibacterial activity of florfenicol was enhanced during the production of florfenicol composite nanogels. This may also be due to the addition of chitosan. Chitosan has antibacterial activity [12]. The time-killing

https://doi.org/10.4142/jvs.22046

curves and live/dead bacterial staining showed that florfenicol composite nanogels had more potential antibacterial activity against SCVs than florfenicol solution. Moreover, the bactericidal ability of florfenicol solution and florfenicol composite nanogels also increased with increasing drug concentration. This suggests that the effect of the florfenicol solution and florfenicol composite nanogels against the SCV strains was concentration-dependent. Thus, the area under the concentration-time curve/minimum inhibitory concentration (MIC) might be a more appropriate parameter to formulate the dosage regimen of florfenicol composite nanogels against SCVs [29]. Furthermore, the therapeutic experiments suggested that the florfenicol composite nanogels had an excellent therapeutic effect (80%) on mouse SCVs mastitis than the florfenicol solution (76.6%). This may be attributed to the following three reasons. 1) CS has an antibacterial effect. When used as hydrogel excipients, it may improve the antibacterial activity of florfenicol and the therapeutic effect. 2) The cure rate of florfenicol composite nanogels was increased because of the sustained-release performance. 3) The antibacterial activity of florfenicol was enhanced during the production of florfenicol composite nanogels. Thus, the florfenicol composite nanogels were more advantageous than the florfenicol solution for treating cow mastitis caused by SCV strains. The biosafety studies showed that florfenicol-loaded CS-TPP composite nanogels had no obvious side effects or toxic implications (especially mammary gland, liver, kidney, and blood), and it had a practical application prospect. Overall, the prepared florfenicol-loaded CS-TPP composite nanogels had an ideal therapeutic effect against cow mastitis caused by SCV strains.

In this study, novel florfenicol-loaded CS-TPP composite nanogels were successfully prepared by ionic gelation to improve their therapeutic concentrations and residence time, ensuring the target delivery to the SCV-infected site. The results suggested that florfenicol composite nanogels have obvious sustained-release performances in pH 5.5. More importantly, the designed florfenicol composite nanogels had a stronger antibacterial activity against SCVs than the florfenicol solution. On the other hand, it had an excellent therapeutic potential on mouse SCVs mastitis. Moreover, the prepared florfenicol composite nanogels had no side effects or toxicity and have practical application prospects. Therefore, the present study may provide a strategy to enhance the therapeutic efficacy of florfenicol against cow mastitis caused by SCV strains.

REFERENCES

1. Fung-Tomc J, Kolek B, Bonner DP. Ciprofloxacin-induced, low-level resistance to structurally unrelated antibiotics in *Pseudomonas aeruginosa* and methicillin-resistant Staphylococcus aureus. Antimicrob Agents Chemother. 1993;37(6):1289-1296.
PUBMED | CROSSREF
2. Sommerhäuser J, Kloppert B, Wolter W, Zschöck M, Sobiraj A, Failing K. The epidemiology of *Staphylococcus aureus* infections from subclinical mastitis in dairy cows during a control programme. Vet Microbiol. 2003;96(1):91-102.
PUBMED | CROSSREF
3. Algharib SA, Dawood A, Xie S. Nanoparticles for treatment of bovine *Staphylococcus aureus* mastitis. Drug Deliv. 2020;27(1):292-308.
PUBMED | CROSSREF
4. Foster TJ. The *Staphylococcus aureus* "superbug". J Clin Invest. 2004;114(12):1693-1696.
PUBMED | CROSSREF
5. Zhou K, Li C, Chen D, Pan Y, Tao Y, Qu W, et al. A review on nanosystems as an effective approach against infections of *Staphylococcus aureus*. Int J Nanomedicine. 2018;13:7333-7347.
PUBMED | CROSSREF

6. Luo W, Liu J, Zhang S, Song W, Algharib SA, Chen W. Enhanced antibacterial activity of tilmicosin against *Staphylococcus aureus* small colony variants by chitosan oligosaccharide-sodium carboxymethyl cellulose composite nanogels. J Vet Sci. 2022;23(1):e1.
PUBMED | CROSSREF
7. von Eiff C, Becker K, Metze D, Lubritz G, Hockmann J, Schwarz T, et al. Intracellular persistence of *Staphylococcus aureus* small-colony variants within keratinocytes: a cause for antibiotic treatment failure in a patient with Darier's disease. Clin Infect Dis. 2001;32(11):1643-1647.
PUBMED | CROSSREF
8. Blickwede M, Valentin-Weigand P, Rohde M, Schwarz S. Effects of subinhibitory concentrations of florfenicol on morphology, growth, and viability of *Staphylococcus aureus*. J Vet Med B Infect Dis Vet Public Health. 2004;51(6):293-296.
PUBMED | CROSSREF
9. Smith GW, Gehring R, Craigmill AL, Webb AI, Riviere JE. Extralabel intramammary use of drugs in dairy cattle. J Am Vet Med Assoc. 2005;226(12):1994-1996.
PUBMED | CROSSREF
10. Algharib SA, Dawood A, Zhou K, Chen D, Li C, Meng K, et al. Designing, structural determination and biological effects of rifaximin loaded chitosan- carboxymethyl chitosan nanogel. Carbohydr Polym. 2020;248:116782.
PUBMED | CROSSREF
11. Liu J, Ju M, Guan D, Song W, Algharib S, Luo W. Composite inclusion complexes containing sodium alginate composite nanogels for pH-responsive valnemulin hydrochloride release. J Mol Struct. 2022;1263:133054.
CROSSREF
12. Liu Y, Chen D, Zhang A, Xiao M, Li Z, Luo W, et al. Composite inclusion complexes containing hyaluronic acid/chitosan nanosystems for dual responsive enrofloxacin release. Carbohydr Polym. 2021;252:117162.
PUBMED | CROSSREF
13. Kalam MA. The potential application of hyaluronic acid coated chitosan nanoparticles in ocular delivery of dexamethasone. Int J Biol Macromol. 2016;89:559-568.
PUBMED | CROSSREF
14. Algharib S, Dawood A, Zhou K, Chen D, Li C, Meng K, et al. Preparation of chitosan nanoparticles by ionotropic gelation technique: effects of formulation parameters and *in vitro* characterization. J Mol Struct. 2022;1252:132129.
CROSSREF
15. Ikram R, Mohamed Jan B, Abdul Qadir M, Sidek A, Stylianakis MM, Kenanakis G. Recent advances in chitin and chitosan/graphene-based bio-nanocomposites for energetic applications. Polymers (Basel). 2021;13(19):3266.
PUBMED | CROSSREF
16. Agnihotri SA, Mallikarjuna NN, Aminabhavi TM. Recent advances on chitosan-based micro- and nanoparticles in drug delivery. J Control Release. 2004;100(1):5-28.
PUBMED | CROSSREF
17. Muxika A, Etxabide A, Uranga J, Guerrero P, de la Caba K. Chitosan as a bioactive polymer: processing, properties and applications. Int J Biol Macromol. 2017;105(Pt 2):1358-1368.
PUBMED | CROSSREF
18. Wang X, Wang S, Zhang Y. Advance of the application of nano-controlled release system in ophthalmic drug delivery. Drug Deliv. 2016;23(8):2897-2901.
PUBMED | CROSSREF
19. Sharaf OM, Al-Gamal MS, Ibrahim GA, Dabiza NM, Salem SS, El-Ssayad MF, et al. Evaluation and characterization of some protective culture metabolites in free and nano-chitosan-loaded forms against common contaminants of Egyptian cheese. Carbohydr Polym. 2019;223:115094.
PUBMED | CROSSREF
20. Alkasir R, Liu X, Zahra M, Ferreri M, Su J, Han B. Characteristics of Staphylococcus aureus small colony variant and its parent strain isolated from chronic mastitis at a dairy farm in Beijing, China. Microb Drug Resist. 2013;19(2):138-145.
PUBMED | CROSSREF
21. Wang XF, Zhang SL, Zhu LY, Xie SY, Dong Z, Wang Y, et al. Enhancement of antibacterial activity of tilmicosin against Staphylococcus aureus by solid lipid nanoparticles *in vitro* and *in vivo*. Vet J. 2012;191(1):115-120.
PUBMED | CROSSREF
22. Brakstad OG, Aasbakk K, Maeland JA. Detection of Staphylococcus aureus by polymerase chain reaction amplification of the nuc gene. J Clin Microbiol. 1992;30(7):1654-1660.
PUBMED | CROSSREF

23. Tong J, Hou X, Cui D, Chen W, Yao H, Xiong B, et al. A berberine hydrochloride-carboxymethyl chitosan hydrogel protects against *Staphylococcus aureus* infection in a rat mastitis model. Carbohydr Polym. 2022;278:118910.
PUBMED | CROSSREF

24. Suo H, Hussain M, Wang H, Zhou N, Tao J, Jiang H, et al. Injectable and pH-sensitive hyaluronic acid-based hydrogels with on-demand release of antimicrobial peptides for infected wound healing. Biomacromolecules. 2021;22(7):3049-3059.
PUBMED | CROSSREF

25. Grimaudo MA, Concheiro A, Alvarez-Lorenzo C. Nanogels for regenerative medicine. J Control Release. 2019;313:148-160.
PUBMED | CROSSREF

26. van de Manakker F, Vermonden T, van Nostrum CF, Hennink WE. Cyclodextrin-based polymeric materials: synthesis, properties, and pharmaceutical/biomedical applications. Biomacromolecules. 2009;10(12):3157-3175.
PUBMED | CROSSREF

27. Zhou K, Wang X, Chen D, Yuan Y, Wang S, Li C, et al. Enhanced treatment effects of tilmicosin against *Staphylococcus aureus* cow mastitis by self-assembly sodium alginate-chitosan nanogel. Pharmaceutics. 2019;11(10):524.
PUBMED | CROSSREF

28. Li C, Zhou K, Chen D, Xu W, Tao Y, Pan Y, et al. Solid lipid nanoparticles with enteric coating for improving stability, palatability, and oral bioavailability of enrofloxacin. Int J Nanomedicine. 2019;14:1619-1631.
PUBMED | CROSSREF

29. Luo W, Qin H, Chen D, Wu M, Meng K, Zhang A, et al. The dose regimen formulation of tilmicosin against *Lawsonia intracellularis* in pigs by pharmacokinetic-pharmacodynamic (PK-PD) model. Microb Pathog. 2020;147:104389.
PUBMED | CROSSREF